Spectral Efficiency Improvement of Generalized Frequency Division Multiplexing with a Massive Multiple Input Multiple Output System for Next Generation Wireless Communication Networks

Irfan Khan
Department of Electronics and Communication Engineering, Oriental University Indore, India
knirfan@rediffmail.com (corresponding author)

Vikas Tiwari
Department of Electronics and Communication Engineering, Oriental University Indore, India
dr.vikastiwari@orientaluniversity.in

Received: 2 December 2025 | Revised: 3 January 2026, 20 January 2026, and 28 January 2026 | Accepted: 29 January 2026

 DOI: https://doi.org/10.48084/etasr.16649

ABSTRACT

To meet the high throughput and low latency demands of future generations (5G and beyond), many researchers propose improving system performance. As spectral scarcity becomes a defining constraint for future generation wireless networks, the adoption of spectrally efficient waveforms is crucial. In view of this, the current paper discusses a scheme that combines massive Multiple Input Multiple Output (MIMO) and Generalized Frequency Division Multiplexing (GFDM) with a higher-order modulation system. While higher-order modulation in traditional MIMO systems often degrades the error rate, the proposed MIMO GFDM scheme utilizes superior pulse shaping, channel coding, and the massive MIMO system to maintain reliability. The findings confirm that the proposed scheme provides enhanced array gain and spectral efficiency, making it highly effective for next-generation high-capacity networks. Ultimately, a new MIMO GFDM scheme is proposed to integrate these benefits, demonstrating superior performance by simultaneously improving both Symbol Error Rate (SER) and capacity over next generation communication systems. This work evaluates the performance of GFDM against Orthogonal Frequency Division Multiplexing (OFDM) within a massive MIMO downlink framework. Through simulations with eight transmitting antennas and sixteen receiving antennas, utilizing an 8x16 antenna configuration, the spectral efficiency of both waveforms under different modulation orders and channel conditions is evaluated. Simulation results demonstrate that while both systems benefit from the array gain provided by receive diversity, the proposed MIMO GFDM system yields superior throughput in bandwidth-limited regimes. Specifically, GFDM achieves a saturation spectral efficiency of 4.75 bits/s/Hz using QAM 1024, outperforming the OFDM baseline of 4.2 bits/s/Hz by approximately 13%. This performance enhancement is attributed to the block-based filtering structure of GFDM, which significantly reduces the Cyclic Prefix (CP) overhead relative to OFDM. Furthermore, the analysis identifies precise SNR thresholds for link adaptation, confirming that MIMO GFDM is a robust and highly efficient candidate for future high throughput communication systems.

Keywords-massive MIMO; GFDM; OFDM; BER; spectral efficiency

I. INTRODUCTION

The objectives driving the development of upcoming communication systems are to improve spectrum efficiency, enhance transmission capacity, minimize system complexity, and achieve a more robust communication link against channel impairments. Orthogonal Frequency Division Multiplexing (OFDM) offers high effectiveness against channel frequency selectivity because its relatively long symbol time is paired with a Cyclic Prefix (CP) [1]. However, a key limitation of OFDM is its high PAPR and its tendency to produce significant Out-of-Band (OOB) emissions. To overcome these snags, various novel waveforms have been proposed for next generation wireless communication systems, including Filter Bank Multi Carrier (FBMC) [2], Universal Filtered Multi

Carrier (UFMC) [3], and Generalized Frequency Division Multiplexing (GFDM) [4].

The technology employed in this paper is GFDM, a multicarrier modulation scheme. GFDM is distinct because it uses non-rectangular pulse filters and implements a DFT filter bank structure through cyclic convolution in the frequency domain. It enhances spectrum efficiency by requiring less CP and by utilizing non-rectangular filters. GFDM effectively mitigates the issues associated with traditional rectangular pulse filters, specifically a high PAPR [5] and excessive OOB emissions [6]. GFDM is a novel concept that extends and generalizes traditional OFDM. It employs a filtered multi-carrier approach to achieve greater flexibility, making it highly relevant for future cellular systems. GFDM operates by modulating independent blocks, each containing multiple subcarriers and sub symbols. Each subcarrier is shaped using a prototype filter that is circularly shifted in both the time and frequency domains. This filtering action significantly diminishes OOB emissions. The specific process facilitates the use of split spectrum and enables dynamic spectrum distribution, while ensuring minimal intrusion on supplementary services. The implementation of subcarrier filtering might result in non-orthogonal subcarriers, raising the possibility of both Inter Symbol Interference (ISI) and Inter Carrier Interference (ICI). These issues can be effectively alleviated using efficient receiver techniques. A major advantage of GFDM is its reduced overhead; only a single CP is added for a complete block of multiple sub symbols, which in turn helps to boost the spectral efficiency of the system [7].

Another technology for enhancing system performance is the use of a huge number of antennas at the Base Station (BS), a configuration known as large scale MIMO or massive MIMO [8]. The massive MIMO system is an extension of the conventional MIMO system [9]. The ability of MIMO systems to boost transmission capacity makes them suitable for addressing the requirements of high data rate applications. MIMO systems are essential for improving a channel's noise and interference performance. Their use in wireless communications has been instrumental in overcoming several challenges, like fading and multipath effects [10].

Conventional MIMO systems typically limit the antenna count to a maximum of 8 elements at both the transmitter and receiver (e.g., an 8×8 configuration). Massive MIMO significantly escalates the scale of antenna arrays. Depending on the design, BSs can be equipped with as many as 256 antennas, whereas User Equipment (UE) may incorporate up to 32 antennas. That substantial upsurge in antenna elements enhances both throughput and coverage within cellular networks. Furthermore, massive MIMO utilizes its multiple antennas to implement beamforming, which concentrates radio energy into specific directions. This technique is significant for compensating for the greater path loss occurring at an ultra-high frequency. By focusing the radio energy into narrower angular sectors, beamforming significantly boosts spectral efficiency [11].

In 2010, massive MIMO was proposed by Marzetta, a scientist at Bell Labs, focusing on its application in multi-cell environments using a Time Division Duplex (TDD) operational scheme [12]. Introduced in Release 8, the simplest MIMO implementation is the Single User MIMO (SU-MIMO), which employs multiple antennas together with a BS and UE. This configuration allows for various transmission modes that adapt to channel conditions. The two main techniques employed are transmit diversity and spatial multiplexing. Transmit diversity involves simultaneously sending the same data over multiple antennas, which is used primarily to improve the SNR. Conversely, spatial multiplexing employs each antenna to send an independent data stream, thereby increasing the overall system capacity [13].

Single user MIMO, currently used in LTE networks, places a significant computational burden on the UE receiver. The receiver's complexity stems from its need to distinguish the multiple received data streams, which appear as interference. Specifically, to establish channel knowledge, the UE must first decode preamble or pilot data and then perform computationally intensive tasks like calculating the inverse channel matrix to decode the signals. This substantial computational demand is often inefficient for battery-constrained mobile devices. To address this limitation, Multi-User MIMO (MU-MIMO) capitalizes on the BS's greater computational power by moving some of the processing complexity to the BS. The BS accomplishes this by applying a pre-weighting matrix to the data streams at the transmitter side, thereby simplifying the decoding process required at the UE [14].

Massive MIMO is set to significantly increase mobile network capacity through spatial multiplexing while simultaneously improving radiated energy efficiency. Besides, the use of precise beamforming enables the system to focus energy exclusively on target terminals, effectively suppressing interference and mitigating signal fading dips [15]. Beamforming is crucial for a cellular system because it allows the BS to achieve different SINR levels for various users within the same cell [16]. Beamforming significantly diminishes unused transmission power across the coverage area. This concerted transmission indeed lowers inter-cell and intra-cell interference for other users. The enhanced signal superiority and condensed interference, achieved through beamforming, combine with spatial multiplexing to dramatically increase spectral efficiency. Eventually, the efficient use of power and the gain from higher spectral efficiency contribute to important overall power savings at the BS [17].

The Channel State Information (CSI) describes the current quality and features of the wireless channel. Based on this channel assessment, the CSI report proposes the optimal precoding matrix or vector for the BS to use. By providing this information, the network can adjust its transmission to maximize the received signal quality and minimize interference [18]. To estimate downlink CSI, the UE measures the signal quality of the downlink reference signals (pilots) transmitted by the BS [19].

GFDM is being considered a potential digital multicarrier modulation scheme for next generation wireless communication systems because of its inherent flexibility in meeting the standard's diverse requirements. This flexibility is significantly enhanced by its capability to use both orthogonal

and non-orthogonal filters as the prototype filter during the filtering process [20].

Surrogate Model Assisted Differential Evolution for Antenna Synthesis (SADEA) functions as an intellectual, high-speed optimization engine for antenna design [21].

To address the limitations of traditional equalization schemes in high-density networks, authors in [22] proposed a novel iterative Frequency Domain Equalization (FDE) algorithm, specifically for uplink MIMO GFDM systems. Authors in [23] addressed the high detection complexity of MIMO GFDM systems caused by multi-dimensional interference. Authors in [24] investigated detection strategies for MIMO GFDM IM systems to enhance spectral and energy efficiency. Authors in [25] introduced a low complexity approximation for iterative MMSE PIC detection, specifically designed for non-orthogonal waveforms with localized ICI. Authors in [26] evaluated the performance of MIMO GFDM with spatial multiplexing within an LTE-A framework. It was emphasized that GFDM's reduced OOB emissions can be further minimized via Guard Symbols (GS) and pinching the block boundary. To validate theoretical diversity gains in realistic environments, authors in [26] implemented a 2x2 MIMO GFDM system. By testing in real-world environments rather than solely relying on simulations, they verified that the complexity of GFDM is manageable on current hardware, while confirming its superior spectral properties and low latency performance. Furthermore, 6G networks aim to overcome traditional limitations like heterogeneous communication that 5G could not fully resolve. GFDM is emerging as a strong candidate to address these impairments due to its flexible time-frequency structure [27].

Although the individual benefits of MIMO and GFDM are well-documented, prior works limit analysis to low-order constellations and small-scale MIMO. The comparative analysis of their joint performance under massive antenna configurations remains limited. The present paper bridges this gap by evaluating the spectral efficiency of an 8x16 MIMO GFDM system against a conventional MIMO OFDM baseline. This study has rigorously analyzed the impact of different modulations (up to 1024 QAM) and varying SNR on system throughput. The obtained results quantify the specific gain provided by the reduced overhead of GFDM and establish optimal SNR thresholds for link adaptation in future high-density networks.

II. METHOD

The block diagram of the proposed communication system using GFDM and massive MIMO is shown in Figure 1. Binary data (b) from a source are initially encoded to produce the bit sequence (b_T). A mapper, namely Quadrature Amplitude Modulation (QAM), then translates these encoded bits into complex valued symbols chosen from a 2^M point constellation, where M is the order of modulation. The resulting output sequence of the mapper is denoted by the data block vector d, which contains N total symbols. This block is structured across two dimensions. The data are organized into a block composed of K subcarriers and S sub-symbols, resulting in a total of N = K.S symbols. Every individual division $d_{k,s}$ corresponds to the symbol conveyed on the kth subcarrier and through the s^{th} sub-symbol of the block. Each of these symbols modulates a specific prototype filter, $g_{K,S}[n]$, typically chosen as a Root Raised Cosine (RRC) filter to minimize OOB emissions. The generation of a GFDM signal is mathematically defined as a superposition of multiple pulse shapes that are shifted in both time and frequency. The output of the GFDM transmitter is given by [7]:

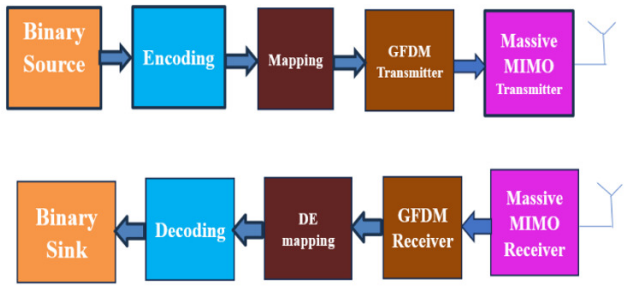

Fig. 1. Block diagram for proposed GFDM system with massive MIMO.

$$x[n] = \sum_{k=0}^{K-1} \sum_{s=0}^{S-1} g_{k,s}[n] d_{k,s} \quad n = 0,1.... N-1 \quad (1)$$

where each $d_{K,S}$ is transmitted after being applied to the equivalent pulse shape filter [9]. The principle of GFDM is the generation of the specific pulse shape for each symbol and subcarrier, designated as $g_{k,s}[n]$, and is given by:

$$g_{K,S}[n] = g\,[(n - sK) \bmod N] \exp[-j2\pi\, k/K.n] \quad (2)$$

where Subcarrier Index (k) belongs to the set of subcarriers (0, 1, ...K-1), Sub symbol Index (s) belongs to the set of time slots (0, 1, ... S-1), and Sample Index (n) belongs to the discrete time samples (0, 1, ...N-1) with $N = K \cdot S$.

This component results from a single prototype filter by imposing two discrete types of shifts. First, a circular time shift is implemented by means of a modulo operation determined by the term (n−sK) mod N. This modulo operation creates a "tail-biting" effect where the end of a filter response wraps around to the beginning of the block, preserving the block structure necessary for efficient equalization. Second, the resulting time-shifted pulse is then modulated by a complex exponential, and this multiplication accomplishes the required frequency shift. Prior to entering the channel, a CP is added to the GFDM signal to prevent ISI.

By employing M transmit antennas in a massive MIMO system, the signal transmitted across all antennas is represented by the vector:

$$R(t) = \left[r_1(t), r_2(t), ...r_m(t)\right]^T \quad (3)$$

The signal transmitted from the m^{th} antenna, denoted as $r_m(t)$, is mathematically represented as the product of the dedicated beamforming weight w_m and the transmitted data signal r(t). This relationship is expressed as:

$$r_m(t) = w_m{}^H r(t) \quad (4)$$

where w_m denotes the beamforming weight vector fed to the m^{th} antenna and superscript H denotes the Hermitian (conjugate transpose) operation.

The signal propagation is modeled as a frequency flat Rayleigh fading channel, appropriate for the rich scattering environment typical of massive MIMO deployments. In a massive MIMO system, the signal received by the m^{th} antenna on the k^{th} subcarrier is given by:

$$Y_{km}(t) = h_{km} Hr(t) + n_{km} \quad (5)$$

where h_{km} is the channel response among the k^{th} subcarrier and the m^{th} receive antenna, n_{km} is the AWGN, which affects transmission on the k_{th} subcarrier and is measured at the m_{th} receive antenna.

Following reception, the primary processing step is to employ 'zero-forcing' equalization to eliminate the linear effects of channel and noise, thereby improving the original transmitted symbols. Following equalization, the estimated signal streams undergo GFDM demodulation. The GFDM demodulation first performs time and frequency synchronization and then discards the CP to eliminate the circular convolution tails. The time-domain signal is then transformed back to the frequency domain via Fast Fourier Transform (FFT). To maximize the SNR and minimize ISI, an RRC filter is applied to the subcarriers. After demodulation, the receiver performs demapping to generate a stream of bits. This sequence is then passed through a channel decoder to retrieve the transmitted binary data. GFDM provides significantly greater degrees of freedom compared to traditional OFDM or Single Carrier Frequency Domain Equalization (SC-FDE). GFDM reduces to OFDM when the number of sub symbols equals 1 and to SC-FDE when the number of subcarriers equals 1. This structure allows for precise spectrum engineering, including per-subcarrier pulse shaping. Consequently, GFDM enables flexible bandwidth configuration, ranging from a large number of narrowband subcarriers (similar to OFDM) to a small number of wideband subcarriers (similar to SC-FDM) without requiring changes to the sampling rate.

A. Performance Metrics

These metrics act as the primary proof of the system's viability.

- Symbol Error Rate (SER): It serves as a significant metric for evaluating the reliability of digital transmission by quantifying the frequency of incorrect symbol detection. The SER exhibits strong resilience against spatial interference while supporting higher order modulation. It is given by [28]:

$$SER = 2\left(p - \frac{1}{p}\right) erfc\left(\sqrt{r}\right) - \left(p - \frac{1}{p}\right)^2 erfc^2\left(\sqrt{r}\right) \quad (6)$$

where $r = \frac{3RT}{2}(2^{\mu} - 1)\frac{Es}{\beta N_0}$, RT = KT/KS + NCP, μ is the number of bits per symbol, K and S denote the number of subcarriers and sub symbols respectively, Es is the average energy per symbol, N_0 is the noise power density, and β is the Noise Enhancement Factor (NEF) which determines the SNR reduction.

- BER: BER is a metric used to quantify the reliability of a data transmission system. It represents the end-to-end performance of the communication link, counting exactly how many individual binary digits (0 s and 1 s) were corrupted during transmission. It is given by:

$$BER = SER/\log_2 M \quad (7)$$

- Capacity: It represents the maximum achievable data rate for error-free transmission over a given communication channel. It acts as the fundamental speed limit of the wireless link. This is mathematically expressed as:

$$Capacity = \eta * \sum_{i=1}^{Nt} \log_2(1 + SNRi) \quad (8)$$

where $\eta = SK/(SK + Ncp)$, S is the number of sub symbols, and K is the number of subcarriers.

- Spectral Efficiency: A key performance metric that evaluates how effectively the available frequency spectrum is utilized to transmit data. The spectral efficiency (measured in bits/s/Hz) is calculated as:

$$\eta = (1 - SER) * \log_2(M) * Code\ Rate \quad (9)$$

B. Flow Chart

This flow chart evaluates the spectral efficiency performance of an 8×16 MIMO-GFDM system under Rayleigh fading using ZF detection, higher order QAM, and channel coding across a wide SNR range.

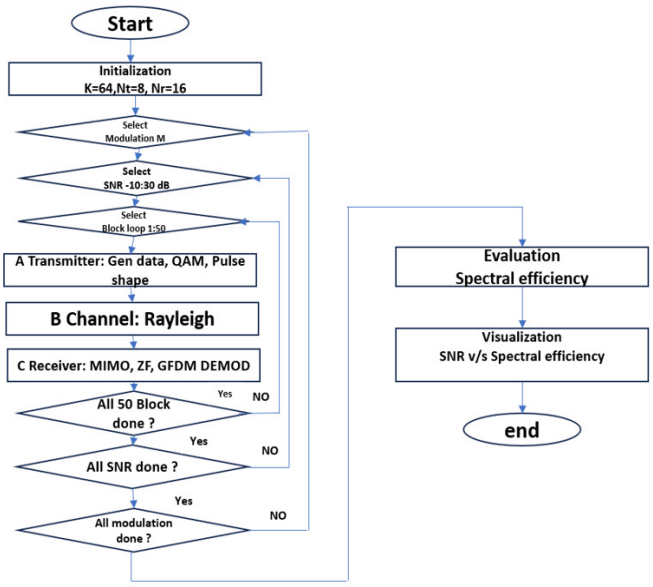

Fig. 2. Flow Chart.

C. Algorithm: MIMO-GFDM Simulation

```
1. Initialization
Define System Parameters:
GFDM: 64 subcarriers (K=64), 4 sub symbols
(S=4). Total samples Ns = 256.
```

```
Modulation: Test loop for Modulation
Orders M = [128, 256, 512, 1024].
Coding: Code Rate (CR) = 1/3.
Cyclic Prefix: 1/8 of symbol length.
MIMO: 8 Transmit Antennas (Nt=8), 16
Receive Antennas (Nr=16).
Simulation: 50 blocks per SNR point, SNR
range −10 dB to 30 dB
2. Main Simulation Loop (Outer Loop:
Modulation Order M)
For each M in [128, 256, 512, 1024]:
Reset: Re-initialize random states to
ensure fair comparison between modulation
orders.
SNR Loop: For each SNR value from −10 to
30 dB:
Block Loop: For 50 iterations:
A. Transmitter:
Source: Generate random integer data
matrix (K* S).
Encoding: Apply Error Encoding to data.
Modulation: Map data to QAM constellations
(qammod).
Pulse Shaping:
Initialize Root Raised Cosine (RRC)
transmit filter (Roll-off = 0.2).
Perform IFFT on modulated data.
Filter the signal using the RRC object.
Cyclic Prefix: Append the last cp samples
to the start of the frame.
B. MIMO Channel:
Channel Matrix: Generate a 16*8 complex
Gaussian channel matrix H (Rayleigh
Fading).
Transmission: Replicate the single
transmitted signal across all 8 transmit
antennas (Diversity/Beamforming mode).
Reception: Multiply channel H by transmit
vector w and add AWGN noise according to
current SNR.
C. Receiver:
MIMO Equalization: Apply Zero Forcing (ZF)
detector:
y = (H^H *H) ^-1*H^H *Received Signal
Combination: Average the equalized streams
to get a single signal estimate.
GFDM Demodulation:
Filter signal with RRC Receive Filter.
Remove transient samples (hard coded
slicing).
Perform FFT.
Decoding: Demodulate QAM symbols and apply
Error Decoding.
Error Check: Compare sent vs. received
data to count errors.
Calculate SER: Average the symbol errors
over the 50 blocks.
3. Performance Evaluation & Plotting
Smooth Data: Apply a moving average
(window size 8) to the SER results.
Calculate Spectral Efficiency:
η= (1 − SER) *log2(M) * Code Rate
Visualization:
Figure: Plot Spectral Efficiency vs. SNR
(Linear Scale).
Add legends dynamically based on M values.
```

D. Complexity Analysis

The computational complexity of multicarrier systems scales significantly during the transition from standard orthogonal waveforms to non-orthogonal, multi-antenna architectures. OFDM represents the baseline for low complexity; its strict orthogonality allows for efficient modulation via FFT and simple single-tap equalization at the receiver, with complexity scaling logarithmically as K log K. In contrast, GFDM improves spectral efficiency by reducing CP overhead but incurs a higher computational cost due to its non-orthogonal nature. When spatial multiplexing is introduced, MIMO OFDM requires matrix inversion for each subcarrier independently, increasing complexity linearly with the number of subcarriers and cubically with the number of antennas. Finally, MIMO GFDM stands as the most computationally intensive architecture among the four, combining the challenges of both spatial multiplexing and non-orthogonal waveforms.

III. SIMULATION RESULTS

The simulation is driven by a range of parameters and computational techniques using MATLAB. The key parameters are listed in Table I.

TABLE I. SIMULATION PARAMETERS

Parameter	Description
GFDM filter	RRC filter
Roll-off factor	0.2
Channel	Rayleigh
No. of transmitting antennas	8
No. of receiving antennas	16,32,64,128
Modulation	QAM 512
Coding	Turbo code
BW	20 MHz

Figure 3 illustrates the BER performance of the massive MIMO system with GFDM for different receiving antennas for various SNRs for QAM 512. The most significant reflection from the graph is the great performance enhancement that comes from increasing the number of receiving antennas from 16 to 128. The BER curves shift sharply to the left, demonstrating that the system accomplishes the same level of reliability with a much lower SNR. This performance gain is extensive; for instance, to sustain a target BER of 10^{-3}, the system with Rx = 16 requires an SNR of approximately 13 dB, while increasing to Rx = 128 decreases the required SNR to only approximately 2 dB. This characterizes how increasing the number of receiving antennas significantly improves the system's ability to combat noise. This characteristic gain in performance is distinctive of communication systems that employ spatial diversity techniques.

The SER versus the number of receiving antennas in a massive MIMO system employing GFDM is depicted in Figure 4. For any fixed number of receiving antennas, increasing the SNR from 2 to 8 steadily decreases the SER, as higher signal quality makes symbol decoding easier. However, the most significant finding is the high performance gain accomplished by cumulatively receiving antennas. This scheme rapidly transitions from a state of high error (SER near 1.0 at 8 antennas) to near-seamless reliability as the number of receiving antennas increases. For instance, the SER drops from 0.4 at 16 antennas (SNR = 8 dB) to approximately zero at 32 antennas and becomes extremely low for all SNRs as the number of receiving antennas reaches 64 or 128. This illustrates the powerful effectiveness of receiver diversity and massive MIMO principles, showing that upsurging the number of receiving antennas is highly effective at reducing SER, even in noisy, low-SNR conditions, and highlights the system's strong noise rejection capability and scalability.

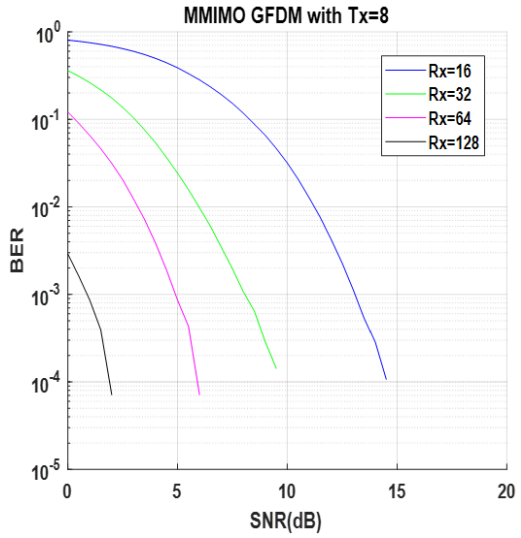

Fig. 3. BER performance of massive MIMO GFDM system for different receiving antennas (Rx) for QAM 512.

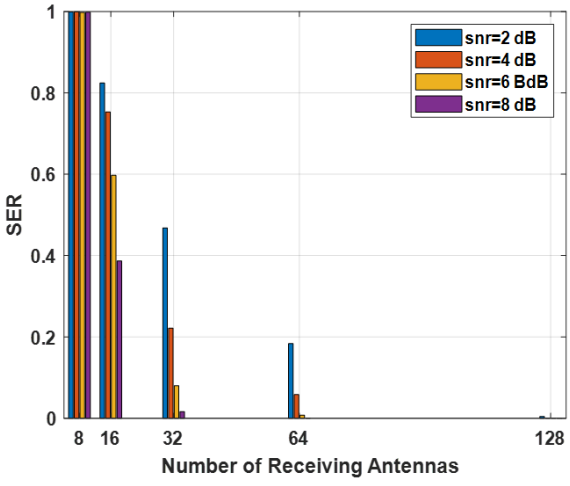

Fig. 4. SER performance of massive MIMO GFDM system.

Figure 5 displays the capacity of the massive MIMO GFDM system with QAM 512 for different SNR and Rx (number of receiving antennas). The most significant finding is how the system parameter Rx affects spectral efficiency. As Rx increases from 16 to 128, the capacity curves shift vividly to the left, signifying a faster saturation. This shift means that the system can achieve its near-maximum capacity with a significantly lower SNR. The Rx = 16 configuration requires approximately 12 dB of SNR, while the Rx = 128 configuration requires only around 4 dB of SNR. This analysis demonstrates the principle of MIMO spatial multiplexing gain, confirming that increasing the number of receiving antennas effectively enhances capacity by improving channel quality, allowing the system to reach high data rates much faster and making the communication link far more power-efficient.

Figure 6 illustrates the spectral efficiency of the 8x16 MIMO OFDM system as a function of the SNR. The system performance is evaluated across a range of modulation orders. As observed, the spectral efficiency exhibits a nonlinear dependency on SNR, characterized by distinct performance regimes dictated by the modulation order. In the low SNR regime (SNR<12dB), lower order modulation schemes (M=128) outperform higher order constellations. This behavior is attributed to the larger Euclidean distance between constellation points in lower order schemes, which ensures greater robustness against noise-induced symbol errors and maintains link stability under adverse channel conditions. Conversely, higher modulation orders, such as M=1024, exhibit negligible throughput in this region due to severe SER. As channel conditions improve (SNR>15dB), the performance curves intersect, indicating the transition points where the benefits of increased bit density outweigh the SNR consequence. In the high SNR regime, the system becomes bandwidth-limited rather than power limited. Consequently, the M=1024 achieves the saturation level of approximately 4.2 bits/s/Hz. The saturation levels for each curve align with the theoretical maximum throughput limits imposed by the respective modulation order. The steep gradient of the efficiency curves reflects the significant array gain provided by the 16 receiving antennas, which effectively mitigates the fading effects.

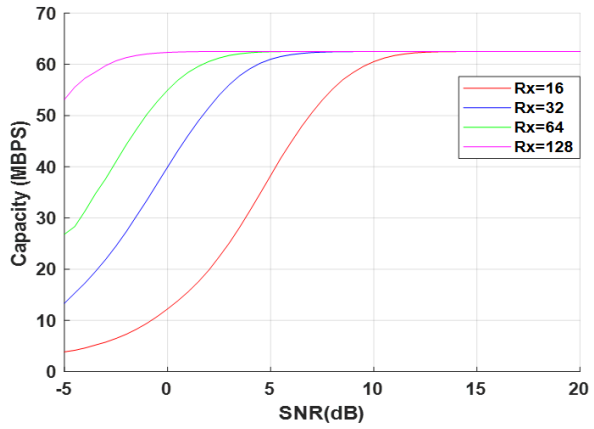

Fig. 5. Capacity of massive MIMO GFDM system for different receiving (Rx) antennas for QAM 512.

Table II presents a comparison between the existing MIMO OFDM system and the proposed MIMO GFDM system.

Figure 7 exhibits the spectral efficiency of the 8x16 MIMO GFDM system. This plot reveals the performance superiority of GFDM over the OFDM system, specifically in terms of maximum throughput due to the reduced CP overhead. The steep slope of the curves in the 5-12 dB range highlights the effective interference cancellation provided by the massive receiver array (Rx=16), validating the feasibility of higher order modulations even in non-orthogonal waveform circumstances.

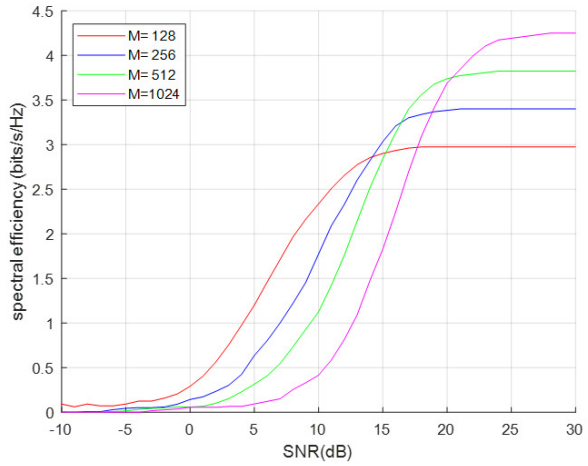

Fig. 6. Spectral efficiency of the 8x16 MIMO OFDM system.

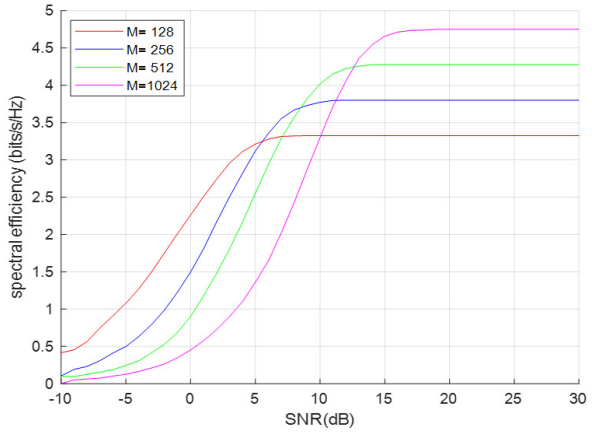

Fig. 7. Spectral efficiency of the 8x16 MIMO GFDM system.

A direct comparison between the OFDM (Figure 6) and GFDM (Figure 7) reveals an important improvement in spectral efficiency exhibited by the GFDM waveform. While both systems exhibit similar trends in the power limited regime (SNR < 5dB), significant divergence is observed in the saturation levels at high SNR. Specifically, for higher order modulation M=1024, the GFDM system achieves a peak spectral efficiency of approximately 4.75 bits/s/Hz, whereas the OFDM counterpart saturates at 4.2 bits/s/Hz. This represents a throughput enhancement of approximately 13%. This gain is intrinsically linked to the block-based filtering structure of GFDM, by appending a single CP for an entire block of sub symbols rather than one per individual symbol as in OFDM. As a result, the GFDM transceiver significantly reduces redundancy overhead. Consequently, the proposed MIMO GFDM effectively maximizes the utilization of the available bandwidth, offering a superior solution for high throughput scenarios where spectral resources are scarce, validating it as a potential candidate for 6G backhaul.

This specific configuration, the 8x16 MIMO with short block GFDM (S=4) and higher order modulation (up to 1024 QAM), represents a high throughput, low latency scenario typical of 5G/6G Ultra Reliable Low Latency Communications (URLLC) or backhaul links.

TABLE II. PERFORMANCE COMPARISON OF MIMO OFDM AND MIMO GFDM (Tx=8 AND Rx=16)

Parameter	MIMO OFDM (baseline)	MIMO GFDM (proposed)	Improvement
Maximum spectral efficiency (1024)	Approx. 4.25	Approx. 4.75	13%
CP overhead	High (1 CP per symbol)	Low (1 CP per block)	Reduced redundancy
Saturation SNR regime	> 25 dB	> 15 dB	Reaches max speed earlier
Link adaptation threshold (128 to 256)	Approx 12 dB	Approx 6 dB	6 dB gain (more robust)

IV. CONCLUSION

This paper has presented a comprehensive performance analysis of the 8×16 Multiple Input Multiple Output (MIMO) Generalized Frequency Division Multiplexing (GFDM) system, benchmarking its spectral efficiency against a conventional MIMO OFDM baseline under varying modulation orders. The results demonstrate that the proposed MIMO GFDM offers a significant throughput advantage in high SNR regimes. Specifically, by amortizing the Cyclic Prefix (CP) overhead across a block of sub symbols, the GFDM system achieves a saturation efficiency of 4.75 bits/s/Hz with Quadrature Amplitude Modulation (QAM) 1024, representing a 13% improvement over the Orthogonal Frequency Division Multiplexing (OFDM) counterpart. Furthermore, the simulation identifies critical SNR crossovers, most notably at 6 dB and 8 dB, which serve as optimal switching thresholds for link adaptation. Simulation results demonstrate that the system accomplishes a substantial reduction in BER as the number of receiving antennas is augmented, illustrating diversity gain inherent to massive MIMO configurations in a GFDM system. The additional receiver diversity provides a substantial gain in terms of the required SNR, which is a key advantage for enabling reliable communication in low power or long-range scenarios. Furthermore, increasing the number of receiving antennas enhances system capacity. This work highlights the practical benefits of scaling up the number of receiving antennas in the massive MIMO technique for achieving robust and high-quality wireless links. These findings confirm that MIMO GFDM, when coupled with massive receive diversity, provides a robust and spectrally efficient solution for next generation

wireless networks, capable of supporting higher order constellations even in the presence of intrinsic self-interference.

DECLARATION OF COMPETING INTERESTS

The authors declare that there is no conflict of interest regarding the publication of this paper.

ACKNOWLEDGMENT

The authors declare that no financial support was received for the research, authorship, or publication of this article from any funding agency in the public, commercial, or any institution. The full publication fees were borne by the authors.

DATA AVAILABILITY

No datasets were utilized in the preparation of this manuscript.

REFERENCES

[1] S. P. Paul and D. Vetrithangam, "A Thorough Assessment on Orthogonal Frequency Division Multiplexing (OFDM) based Wireless Communication: Challenges and Interpretation," in *2023 International Conference on Sustainable Computing and Smart Systems* (*ICSCSS*), Coimbatore, India, June 14–16, 2023, pp. 1145–1151, https://doi.org/10.1109/ICSCSS57650.2023.10169766.

[2] F. Hamdar, C. M. G. Gussen, J. Nadal, C. A. Nour, and A. Baghdadi, "FBMC/OQAM Transceiver for Future Wireless Communication Systems: Inherent Potentials, Recent Advances, Research Challenges," *IEEE Open Journal of Vehicular Technology*, vol. 4, pp. 652–666, Aug. 2023, https://doi.org/10.1109/OJVT.2023.3303034.

[3] F. S. Shawqi, L. Audah, A. T. Hammoodi, M. M. Hamdi, and A. H. MOHAMMED, "A Review of PAPR Reduction Techniques for UFMC Waveform," in *4th International Symposium on Multidisciplinary Studies and Innovative Technologies* (*ISMSIT*), Instabul, Turkey, Oct. 22–24, 2020, pp. 1–6, https://doi.org/10.1109/ISMSIT50672.2020.9255246.

[4] N. Michailow, S. Krone, M. Lentmaier, and G. Fettweis, "Bit Error Rate Performance of Generalized Frequency Division Multiplexing," *in 2012 IEEE Vehicular Technology Conference* (*VTC Fall*), Quebec City, QC, Canada, Sept. 03–06, 2012, pp. 1–5, https://doi.org/10.1109/VTCFall.2012.6399305.

[5] N. Michailow and G. Fettweis, "Low peak-to-average power ratio for next generation cellular systems with generalized frequency division multiplexing," in *2013 International Symposium on Intelligent Signal Processing and Communication Systems*, Naha, Japan, Nov. 12–15, 2013, pp. 651–655, https://doi.org/10.1109/ISPACS.2013.6704629.

[6] M. R. G. Aghdam, R. Abdolee, B. M. Tazehkand, and A. A. Jirdehi, "Out-of-Band Analysis of GFDM Systems Based on Different Self-Interference Types," in *2023 IEEE 13th Annual Computing and Communication Workshop and Conference* (*CCWC*), Las Vegas, NV, USA, March 8–11, 2023, pp. 0301–0305, https://doi.org/10.1109/CCWC57344.2023.10099217.

[7] N. Michailow *et al*., "Generalized Frequency Division Multiplexing for 5th Generation Cellular Networks," *IEEE Transactions on Communications*, vol. 62, no. 9, pp. 3045–3061, Sept. 2014, https://doi.org/10.1109/TCOMM.2014.2345566.

[8] T. Abood, I. Hburi, and H. F. Khazaal, "Massive MIMO: An Overview, Recent Challenges, and Future Research Directions," in *2021 International Conference on Advance of Sustainable Engineering and its Application* (*ICASEA*), Wasit, Iraq, Oct. 27–28, 2021, pp. 43–48, https://doi.org/10.1109/ICASEA53739.2021.9733081.

[9] G. Bauch and A. Alexiou, "MIMO technologies for the wireless future," in *2008 IEEE 19th International Symposium on Personal, Indoor and Mobile Radio Communications*, Cannes, France, Sept. 15–18, 2008, pp. 1–6, https://doi.org/10.1109/PIMRC.2008.4699969.

[10] R. Varshney, P. Jain, and S. Vijay, "Massive MIMO Systems In Wireless Communication," in *2018 2nd International Conference on Micro-Electronics and Telecommunication Engineering* (*ICMETE*), Chaziabad, India, Sept. 20–21, 2018, pp. 39–44, https://doi.org/10.1109/ICMETE.2018.00022.

[11] S. A. Khwandah, J. P. Cosmas, P. I. Lazaridis, Z. D. Zaharis, and I. P. Chochliouros, "Massive MIMO Systems for 5G Communications," *Wireless Personal Communications*, vol. 120, no. 3, pp. 2101–2115, 2021, https://doi.org/10.1007/s11277-021-08550-9.

[12] T. L. Marzetta, "Noncooperative Cellular Wireless with Unlimited Numbers of Base Station Antennas," *IEEE Transactions on Wireless Communications*, vol. 9, no. 11, pp. 3590–3600, Nov. 2010, https://doi.org/10.1109/TWC.2010.092810.091092.

[13] W. Guo, J. Fan, G. Y. Li, Q. Yin, and X. Zhu, "Adaptive SU/MU-MIMO scheduling schemes for LTE-A downlink transmission," *IET Communications*, vol. 11, no. 6, pp. 783–792, 2017, https://doi.org/10.1049/iet-com.2016.0456.

[14] B. Clerckx and C. Oestges, *MIMO Wireless Networks: Channels, Techniques and Standards for Multi-Antenna, Multi-User and Multi-Cell Systems*. Oxford: Academic Press.

[15] F. Rusek *et al*., "Scaling Up MIMO: Opportunities and Challenges with Very Large Arrays," *IEEE Signal Processing Magazine*, vol. 30, no. 1, pp. 40–60, Jan. 2013, https://doi.org/10.1109/MSP.2011.2178495.

[16] C.-Z. Han, L. Xiao, Z. Chen, and T. Yuan, "Co-Located Self-Neutralized Handset Antenna Pairs With Complementary Radiation Patterns for 5G MIMO Applications," *IEEE Access*, vol. 8, pp. 73151–73163, 2020, https://doi.org/10.1109/ACCESS.2020.2988072.

[17] W. Zhang, X. Xia, Y. Fu, and X. Bao, "Hybrid and full-digital beamforming in mmWave Massive MIMO systems: A comparison considering low-resolution ADCs," *China Communications*, vol. 16, no. 6, pp. 91–102, June 2019, https://doi.org/10.23919/JCC.2019.06.008.

[18] Q. Li, A. Zhang, P. Liu, J. Li, and C. Li, "A Novel CSI Feedback Approach for Massive MIMO Using LSTM-Attention CNN," *IEEE Access*, vol. 8, pp. 7295–7302, 2020, https://doi.org/10.1109/ACCESS.2020.2963896.

[19] C. Luo, J. Ji, Q. Wang, X. Chen, and P. Li, "Channel State Information Prediction for 5G Wireless Communications: A Deep Learning Approach," *IEEE Transactions on Network Science and Engineering*, vol. 7, no. 1, pp. 227–236, 2020, https://doi.org/10.1109/TNSE.2018.2848960.

[20] N. Michailow, M. Lentmaier, P. Rost, and G. Fettweis, "Integration of a GFDM secondary system in an OFDM primary system," in *2011 Future Network & Mobile Summit*, Warsaw, Poland, June 15–17, 2011, pp. 1–8.

[21] Y. J. Ntonya, S. Musyoki, and V. Oduol, "Cognitive Non-Orthogonal Multiple Access with Cooperative Relaying and Antenna Optimization using SADEA for Efficient Spectrum Sharing," *Engineering, Technology & Applied Science Research*, vol. 15, no. 3, pp. 22327–22333, June 2025, https://doi.org/10.48084/etasr.10265.

[22] J. Zhong, G. Chen, J. Mao, S. Dang, and P. Xiao, "Iterative Frequency Domain Equalization for MIMO-GFDM Systems," *IEEE Access*, vol. 6, pp. 19386–19395, 2018, https://doi.org/10.1109/ACCESS.2018.2823002.

[23] E. Öztürk, E. Basar, and H. A. Çırpan, "Spatial modulation GFDM: A low complexity MIMO-GFDM system for 5G wireless networks," in *2016 IEEE International Black Sea Conference on Communications and Networking* (*BlackSeaCom*), Varna, Bulgaria, June 06–09, 2016, pp. 1–5, https://doi.org/10.1109/BlackSeaCom.2016.7901544.

[24] M. Matthé, D. Zhang, and G. Fettweis, "Low-Complexity Iterative MMSE-PIC Detection for MIMO-GFDM," *IEEE Transactions on Communications*, vol. 66, no. 4, pp. 1467–1480, Apr. 2018, https://doi.org/10.1109/TCOMM.2017.2782339.

[25] G. Al-Juboori, A. Doufexi, and A. R. Nix, "System level 5G evaluation of MIMO-GFDM in an LTE-A platform," in *24th International Conference on Telecommunications* (*ICT*), Limassol, Cyprus, May 03–05, 2017, pp. 1–5, https://doi.org/10.1109/ICT.2017.7998273.

[26] M. Danneberg *et al*., "Implementation of a 2 by 2 MIMO-GFDM transceiver for robust 5G networks," in *International Symposium on Wireless Communication Systems* (*ISWCS*), Brussels, Belgium, Aug. 25–28, 2015, pp. 236–240, https://doi.org/10.1109/ISWCS.2015.7454336.

[27] R. A. Kumar and K. S. Prasad, "Performance Analysis of GFDM Modulation in Heterogeneous Network for 5G NR," *Wireless Personal Communications*, vol. 116, no. 3, pp. 2299–2319, 2021, https://doi.org/10.1007/s11277-020-07791-4.

[28] S. K. Bandari, A. Drosopoulos, and V. V. Mani, "Exact SER Expressions of GFDM in Nakagami-m and Rician fading channels," in *Proceedings of European Wireless 2015; 21th European Wireless Conference*, Budapest, Hungary, May 20–22, 2015, pp. 1–6.